Science and Innovation of Advanced Materials

The Materials Research Society of Thailand

Research Article

Devolopment of Co-doped Fe_2O_3 Nanoparticles for Electrochemical Supercapacitor

Aridtha Chaloemram*, Asanee Somdee, Surangkana Wanapop

Faculty of Science, Energy, and Environment, King Mongkut's University of Technology North Bangkok Rayong Campus, Rayong 21120, Thailand

* Corresponding author e-mail: s6513021856521@email.kmutnb.ac.th

Received: *May 12th, 2024* | ***Revised:*** *July 10th, 2024* | ***Accepted:*** *July 27th, 2024*

Abstract: Co-doped Fe_2O_3 nanoparticles were synthesized by the co-precipitation method. These crystalline nanostructures were characterized using X-ray powder diffraction (XRD), scanning electron microscopy (SEM), and transmission electron microscope (TEM). The electrochemical characteristics include charge–discharge cycling, which improves the conductivity and capacitance for the high-performance supercapacitor. The CV analysis of the pure Fe_2O_3 and Co-doped Fe_2O_3 electrode was distinctive in the 1 M KOH solution case. The nanoparticle size electrode reveals enhanced specific capacitance compared to Co-doped Fe_2O_3 and Fe_2O_3 to the electrode has a specific capacitance of about 33.50 $F{\cdot}g^{-1}$ and 13.74 $F{\cdot}g^{-1}$ with a scan rate 5 $mV{\cdot}s^{-1}$.

Keywords: Supercapacitor, Co-precipitation method, Electrochemical, Energy storage

1. Introduction

As global demand increases for electrical energy use today, such as in electronic devices, electric vehicles, and households, a new era of energy technology production and storage has come to meet various needs. For the energy storage system, supercapacitors and batteries become a good candidate for electrical energy storage [1]. Today, batteries have been paid good attention in many fields of energy storage due to their large energy storage system and ease of use. Compared to the supercapacitor, the supercapacitor had limited use up until now [2]. The energy density of a supercapacitor is less than that of a battery and other energy storage technology, such as fuel cells. However, the supercapacitor has an advantage in several ways, such as being reusable and having power density over the battery [3-5].

The electrical capacitor is divided into two types: an electrochemical double-layer capacitor EDLC and a pseudocapacitor [6]. The EDLC, where the electrolyte solution is absorbed in two layers on the electrodes when the electrical energy is supplied, while pseudocapacitors store charge on the surface of the electrode like EDLCs. In addition, there is electron transfer, or redox reactions occur within the material used as the electrode [7]. As a result, pseudocapacitors can hold a higher electrical charge density than EDLC [8].

Metal oxide substances containing iron (Fe) as the main component have been paid much attention for use as the supercapacitor application. Because it has a low cost and is less harmful to the environment [9]. In the case of

* The work was presented at The 22nd International Symposium on Eco-materials Processing and Design (ISEPD 2024), 21-24 January 2024

iron oxide nanomaterial, many researchers have been focused on electrochemical energy storage for a few decades [10]. Iron oxide and some deviations, such as forming composite to the carbon materials or doping with other materials, show an excellent supercapacitor performance. Metal-doped Fe_2O_3 supercapacitor electrodes show enhanced capacitance compared to pure Fe_2O_3. This is mainly due to the improved charge storage capability resulting from metal doping. The addition of metals such as cobalt or nickel changes the electronic structure and introduces extra redox reactions, leading to higher specific capacitance, better rate capability, and improved cycling stability [11]. Electrochemical properties play a crucial role in the application of metal oxides, such as Fe_2O_3, in energy storage devices. Co-doped Fe_2O_3 has shown promising potential for enhanced capacity compared to pure Fe_2O_3, primarily due to its lower resistivity [12]. In contrast to earlier research, this study used the co-precipitation method with varying precursor concentrations. This method proved effective in producing significant quantities of substances. Previous research had employed hydrothermal synthesis, which led to the creation of nanocomposites consisting of nickel oxide and cobalt oxide with a layer of iron oxide on the surface.

The present research studied iron oxide and Co-doped iron oxide as materials for supercapacitor electrodes [13-14]. The products were synthesized by the co-precipitation method. The materials were characterized by various X-ray diffraction, scanning electron microscopy, and transmitted electron microscopy [15]. All electrochemical properties related to the supercapacitors were also investigated using the electrodes method and potentiostat [16-17].

2. Methodology

2.1 Materials

Analytical grade chemicals were from ferric nitrate nonahydrate $Fe(NO_3)_3{\cdot}9H_2O$, ferric nitrate nonahydrate Loba Chemie PVT.LTD, $(CH_3COO)_2Co{\cdot}4H_2O$ cobalt (II) acetate Ajax Finechem Pty Ltd., NaOH sodium hydroxide pellets for analysis made in Germany Merck KGaA, 64271 Darmstadt Germany. KOH Supelco potassium hydroxide-pellets for analysis made in Germany Merck KGaA, 64271 Darmstadt Germany.

2.2 Synthesis of Fe_2O_3 and Co doped Fe_2O_3 nanoparticles

Fe_2O_3 was synthesized by the co-precipitation method. Briefly, 2.02 g of $Fe(NO_3)_3{\cdot}9H_2O$ was dissolved in 60 ml of DI water with stirring for 10 min, then 3 M of NaOH was added into the above yellow aqueous solution with stirring for 2 h. The sample was washed with DI water and ethanol and dried at 60 °C for 24 h. The sample was calcined at 500 °C for 2 h. Co-doped Fe_2O_3 nanoparticle was synthesized by the co-precipitation method like Fe_2O_3; only 0.6 g of $(CH_3COO)_2Co{\cdot}4H_2O$ was added to the synthesis.

2.3 Electrochemical study

The working electrode for test electrochemical characterizations as-synthesized materials (80%) were mixed with (10%) carbon black and (10%) PVDF as binder. The uniform slurry of the above material was prepared using N-methyl-2-pyrrolidone (NMP) as solvent. For the electrode system, a uniform layer of slurry was painted on the working electrode. The as-prepared slurry was coated onto a piece of nickel foam (1×2 cm^2) and then dried in a vacuum oven at 110 °C overnight.

3. Results and discussion

Characterization

Figure 1 shows the X-ray diffraction of pure Fe_2O_3 and Co-doped Fe_2O_3. As a result, the peak of pure Fe_2O_3 shows much crystallinity formation, which matches well to the hematite Fe_2O_3 (PDF 00-033-0664). The diffraction peaks located at 32.76°, 35.31°, 43.49°, 49.15°, 53.70°, 56.10°, 63.74° and 77.45° correspond to the (104), (110), (202), (024),

(116), (211), (300) and (306) miller indices. Meanwhile, the Co-doped into the Fe_2O_3 shows a slightly different pattern. The Co-doped Fe_2O_3 shows poor crystallinity when compared to the un-doped. The observed decrease in crystallinity in Co-doped Fe_2O_3 can be attributed to several factors. When cobalt is doped into the Fe_2O_3 lattice, it can distort the crystal structure and lattice parameters due to the difference in ionic radii between iron and cobalt. The quality of the crystals can also be influenced by the concentration of dopants, synthesis methods, and annealing conditions. High dopant concentrations or non-optimal synthesis and annealing processes could result in defects, dislocations, or phase impurities, leading to decreased crystallinity in the doped material [18]. Nevertheless, the main peak position remains the Fe_2O_3. Thus, this evidence reflected to the successfully doped by Co into the parent Fe_2O_3 lattice.

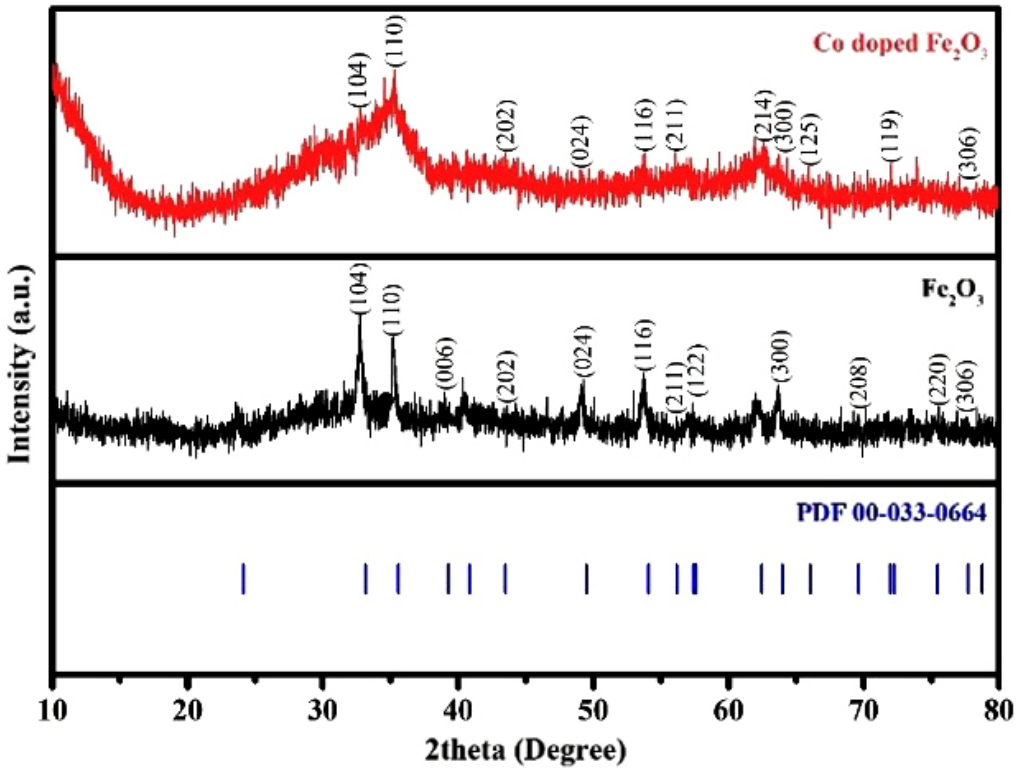

Figure 1 XRD patterns of pure Fe_2O_3 and Co-doped Fe_2O_3.

Figure 2 shows the SEM images of pure Fe_2O_3 and Co-doped Fe_2O_3. In Figure 2(a) SEM images of pure Fe_2O_3 show a Nanostructure where the average particle size is approximately 100 nm in diameter. Figure 2(c) shows the analysis for the elemental composition of materials (or EDS) of Co-doped Fe_2O_3, which confirms the co-existence of iron, oxygen, and cobalt. Figure 3(a) shows the overview, and Figure 3(b) shows the high-resolution TEM images of pure Fe_2O_3. As a clear result, there is one phase belonging to the pure Fe_2O_3. The d-spacing of 1.40 nm is specified to the (125) Miller plane. Figure 3(c) shows the overview, and Figure 3(d) shows HRTEM images. The d-spacing of 1.40 nm is assigned to the (125) of Co-doped Fe_2O_3.

Electrochemical properties

Figure 4 shows the CV of pure Fe_2O_3 and Co-doped Fe_2O_3 at scan rates 5, 10, 25, 50, 75, and 100 $mV{\cdot}s^{-1}$, and compares the pure and doped at scan rates of 5 $mV{\cdot}s^{-1}$. The results indicate that the CV curves of both substances, pure Fe_2O_3 and Co-doped Fe_2O_3, have the shape of a pseudocapacitor. The estimate of the specific capacitance of pure Fe_2O_3 and Co-doped Fe_2O_3 electrodes is in Table 1.

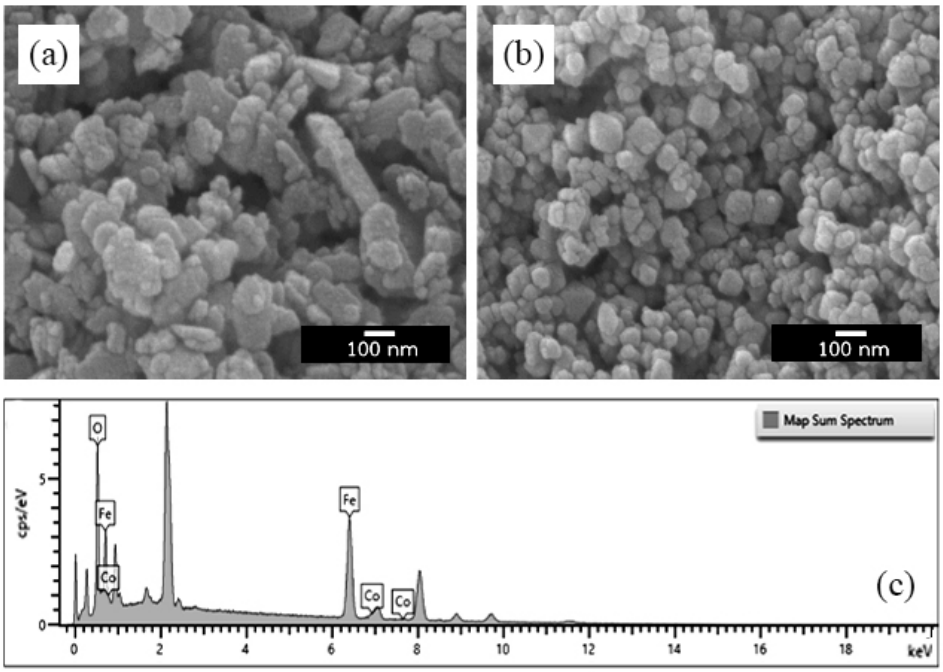

Figure 2 (a) SEM image of pure Fe_2O_3, (b) SEM image of Co-doped Fe_2O_3, and (c) EDS of Co-doped Fe_2O_3.

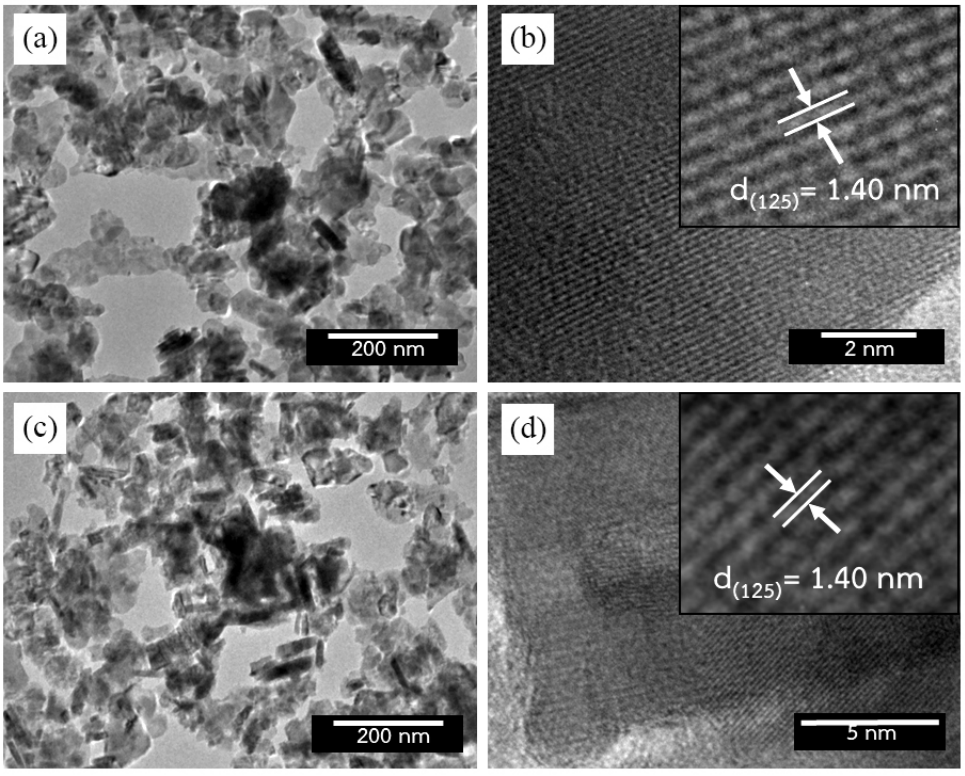

Figure 3 (a) TEM images of pure Fe_2O_3, (b) HRTEM images of Fe_2O_3, (c) TEM images of Co-doped Fe_2O_3, and (d) HRTEM image of Co-doped Fe_2O_3.

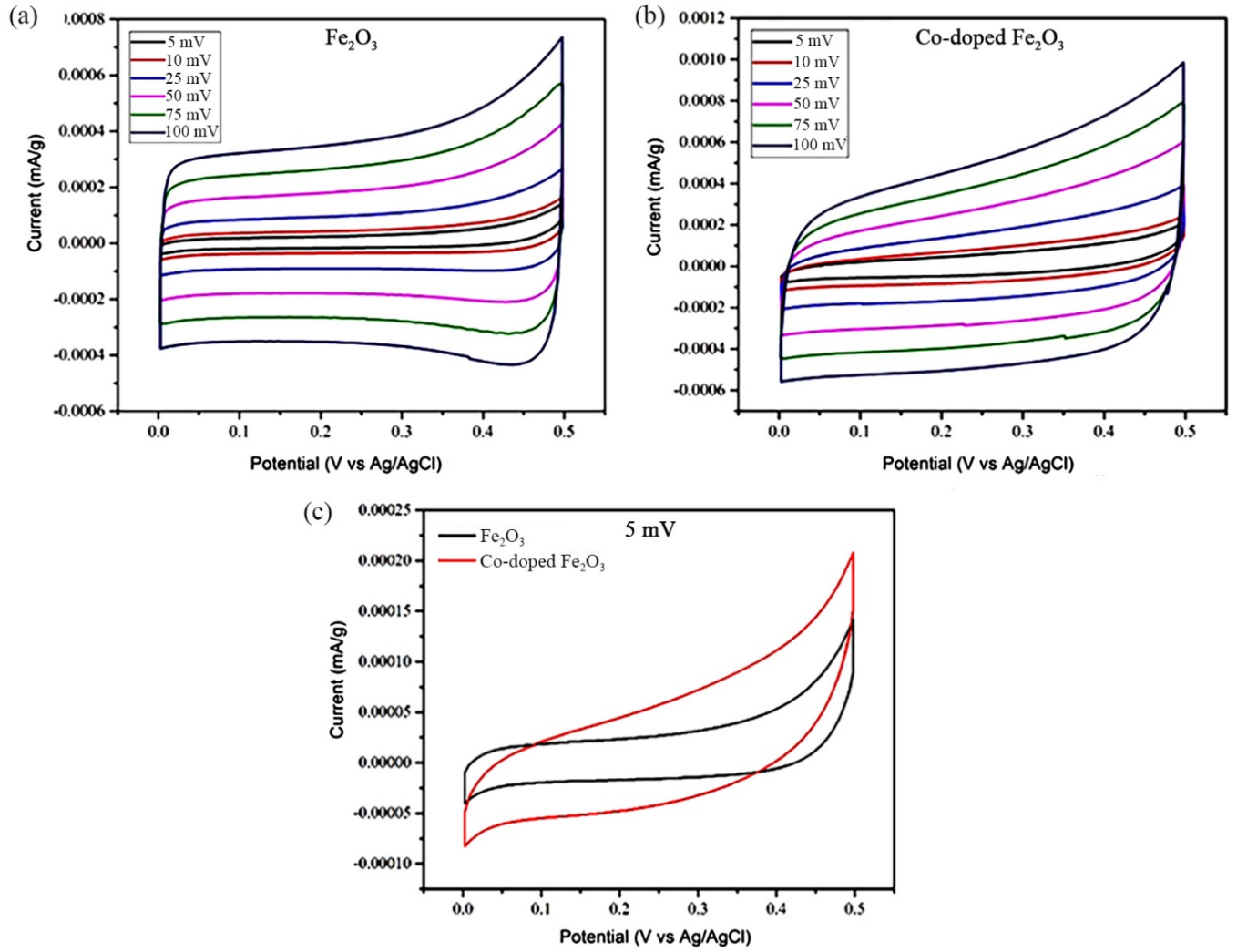

Figure 4 Electrochemical measurements of simple; (a) CV curve of pure Fe_2O_3, (b) CV curve of Co-doped Fe_2O_3, and (c) comparison CV curves of pure and doped at a scan rate of 5 $mV{\cdot}s^{-1}$.

Table 1 Specific capacitance of pure Fe_2O_3 and Co-doped Fe_2O_3 at a scan rate of 5 $mV{\cdot}s^{-1}$

Electrode materials	Capacitance ($F{\cdot}g^{-1}$)
pure Fe_2O_3	13.74
Co-doped Fe_2O_3	33.50

Figure 5 shows the GCD curves of as-synthesized electrodes of pure Fe_2O_3 and Co-doped Fe_2O_3 at applied charge-discharge current density of 0.1 $mA{\cdot}g^{-1}$ within the potential window 0 to 0.5 (V) in 1 M KOH electrolyte. The nonlinear GCD curves indicate the characteristic pseudocapacitive behavior, which can be attributed to the reversible redox reaction with negligible voltage loss. The pseudocapacitive mechanism corroborated the surface intercalation of K^+ ions onto pure Fe_2O_3 lattices. The result indicates that the electrode fabricated from the Co-doped Fe_2O_3 electrode shows a higher discharging time than pure Fe_2O_3.

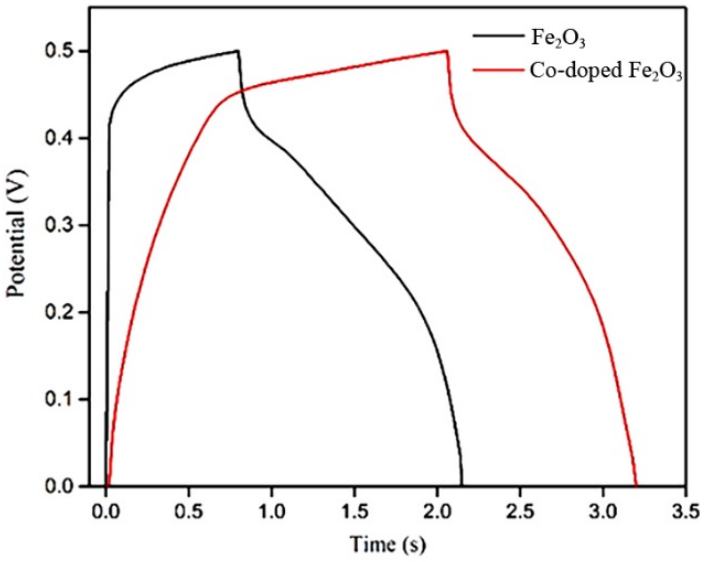

Figure 5 Characteristics of GCD electrode of pure Fe_2O_3 and Co-doped Fe_2O_3 samples at current density 0.1 $mA{\cdot}g^{-1}$.

Figure 6 shows the EIS diagram for materials pure Fe_2O_3 and Co-doped Fe_2O. The latter has the low resistivity. The low resistance value allows the anion flowed through the device [18]. According to this, it will result in a greater capacity value, which can be confirmed by the measured capacity value. In addition, combining cobalt with Fe_2O_3 affects the crystal structure and morphology, resulting in better production capacity. The addition of cobalt can alter the crystal lattice, increase structural stability, and prevent deterioration during cycling. These modifications can help improve the electrical system [19-20]. The addition of cobalt to Fe_2O_3 changes the redox potential and allows for more redox reactions, increasing the charge storage capacity. This process can create new active sites or modify existing ones, leading to improved utilization of redox-active materials and greater capacity [20-21].

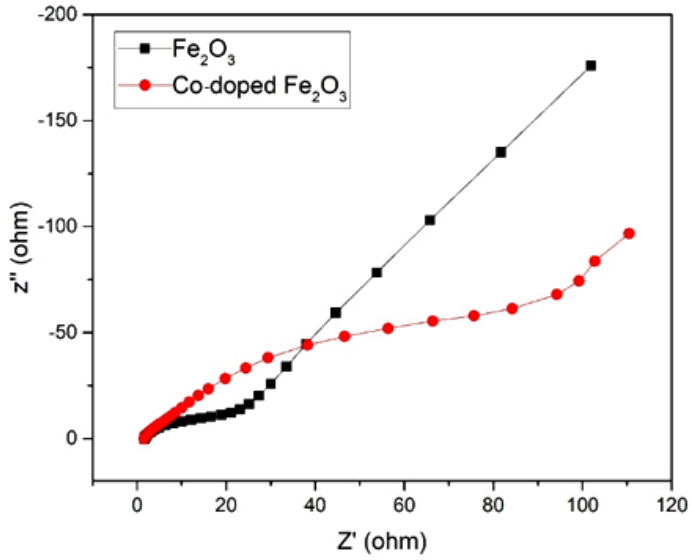

Figure 6 Nyquist plot of two electrodes, pure Fe_2O_3 and Co-doped Fe_2O_3.

4. Conclusion

This work explored the pure Fe_2O_3 and Co-doped Fe_2O_3 nanomaterials for supercapacitor applications. The products were synthesized by the co-precipitation method. The XRD revealed that Fe_2O_3 has a hexagonal hematite phase. At 5% Co doping, the main phase of the material was still similar to the pure phase, implying that the Co atom successfully substituted in the host Fe_2O_3. The electrochemical studies showed the improvement of Co substitution by increasing the specific capacitance of the main Fe_2O_3.

Acknowledgment

This research was funded by King Mongkut's University of Technology North Bangkok. Contract no. KMUTNB-66-KNOW-08.

References

[1] K. Xie, J. Li, Y. Lai, W. Lu, Z. Zhang, Y. Liu, L. Zhou, H. Huang, Highly ordered iron oxide nanotube arrays as electrodes for electrochemical energy storage, *Electrochem. Commun.* **13** (2020) 657-660.

[2] M. Kang, S. Zhou, J. Zhang, F. Ning, C. Ma, Z. Qiu, Facile fabrication of oxygen vacancyrich α-Fe_2O_3 microspheres on carbon cloth as negative electrode for supercapacitors, *Electrochim. Acta* **338** (2020) 135820.

[3] R. Kötz, M. Carlen, Principles and applications of electrochemical capacitors, *Electrochim. Acta* **45** (2000) 2483-2498.

[4] S. Mallick, P. P. Jana, C. R. Raj, Asymmetric supercapacitor based on chemically coupled hybrid material of Fe_2O_3-Fe_3O_4 heterostructure and nitrogen doped reduced graphene oxide, *ChemElectroChem* **5** (2018) 2348-2356.

[5] J. M. Polfus, K. Jayasayee, Robust nanocomposites of α-Fe_2O_3 and N-doped graphene oxide: Interfacial bonding and chemisorption of H_2O, *Carbon* **152** (2019) 497-502.

[6] X. Zhang, H. Liao, X. Liu, R. Shang, Y.Zhou, Y. Zhou, Facile synthesis of Fe_2O_3 nanospheres anchored on oxidized graphitic carbon nitride as a high-performance electrode material for supercapacitors, *Int. J. Electrochem. Sci.* **15** (2020) 2133-2144.

[7] L. Xu, J. Xia, H. Xu, S. Yin, K. Wang, L. Huang, L. Wang, H. Li, Reactable ionic liquid assisted solvothermal synthesis of graphite-like hybridized α-Fe_2O_3 hollow microspheres with enhanced supercapacitive performance, *J. Power Sources* **245** (2020) 866-874.

[8] L. Q. Mai, F. Yang, Y. L. Zhao, X. Xu, L. Xu, Y. Z. Luo, Hierarchical $MnMoO_4$/$CoMoO_4$ heterostructured nanowires with enhanced supercapacitor performance, *Nature Commun.* **2** (2020) 2133-2144.

[9] Z. Song, W. Liu, P. Xiao, Z. Zhao, G. Liu, J. Qiu, Nano-iron oxide (Fe_2O_3)/three-dimensional graphene aerogel composite as supercapacitor electrode materials with extremely wide working potential window, *Mater. Lett.* **145** (2015) 44-47.

[10] N. Wu, Y. R. Shi, C. Ma, X. Zhang, J. M. Zhou, Y Wei, H Liu, Y. Yan, H. T. Liu, High performance nano-α-Fe_2O_3 electrode materials synthesized by facile and green approaches for lithium-ion batteries, *Mater. Lett.* **238** (2019) 155-158.

[11] R. Zboril, M. Mashlan, D. Petridis, Iron (III) oxides from thermal processes synthesis, structural and magnetic properties, Mössbauer spectroscopy characterization and applications, *Chem. Mater.* **14** (2002) 969-982.

[12] M. A. Nassar, S. I. El-dek, W. M. A. E. Rouby, A. G. El-Deen, Highly efficient asymmetric supercapacitor-based on Ni-Co oxides intercalated graphene as positive and Fe_2O_3 doped graphene as negative electrodes, *J. Energy Storage* **44** (2021) 103305.

[13] A. Phakkhawan, P. Suksangrat, P. Srepusharawoot, S. Ruangchai, P. Klangtakai, S. Pimanpang, V. Amornkitbamrung, Reagent-and solvent-mediated Fe_2O_3 morphologies and electrochemical mechanism of Fe_2O_3 supercapacitors, *J. Alloys Compd.* **919** (2022) 165702.

[14] A. G. Kaningini, T. Motlhalamme, K. J. Cloete, G. K. More, K. C. Mohale, M. Maaza, Fe_2O_3 nanoparticles from *Athrixia phylicoides* DC and their effect on *Cicer arietinum* L. growth performance, *Biocatal. Agric. Biotechnol.* **54** (2022) 102948.
[15] L. Chen, D. Liu, P. Yang, Preparation of α-Fe_2O_3/rGO composites toward supercapacitor applications, *RSC Adv.* **9** (2019) 12793.
[16] G. Mummoorthi, S. Shajahan, M. A. Haija, U. Mahalingam, R. Rajendran, Synthesis and characterization of ternary α-Fe_2O_3/NiO/rGO composite for high-performance supercapacitors, *ACS Omega.* **31** (2022) 27390-27399.
[17] T. C. S. Girisun, M. Saravanan, V. R. Soma, Wavelength-dependent nonlinear optical absorption and broadband optical limiting in Au-Fe_2O-rGO nanocomposites, *ACS Appl. Nano Mater.* **11** (2018) 6337-6348.
[18] L. Wu, W. Wang, S. Zhang, D. Mo, X. Li, Fabrication and characterization of Co-Doped Fe_2O_3 spindles for the enhanced photo-Fenton catalytic degradation of tetracycline, *ACS Omega.* **6** (2021) 33717-33727
[19] L. C. Hsu, H. C. Yu, T. H. Chang, Y. Y. Li, Formation of three-dimensional urchin-like α-Fe_2O_3 structure and its field-emission application, *ACS Appl. Mater. Interfaces* **3** (2011) 3084-3090.
[20] G. Tatrari, M. Ahmed, F. U. Shah, Synthesis thermoelectric and energy storage performance of transition metal oxides composites, *Coord. Chem. Rev.* **498** (2024) 215470.
[21] L. Yang, Q. Zhu, K. Yang, X. Xu, J. Huang, H. Chen, H. Wang, A Review on the application of cobalt-based nanomaterials in supercapacitors, *Nanomaterials* **22** (2022) 4065.